Threshold Selection for TOA Estimation Based on Skewness and Kurtosis in 60GHz Ranging System

Ning Du[1*], Hao Zhang[1,2], Tingting Lv[1], and T. Aaron Gulliver[2]

[1]Department of Electrical Engineering, Ocean University of China,Qingdao, P. R. China
[2]Department of Electrical and Computer Engineering, University of Victoria,Victoria, Canada
Email: {duning1010, lvtingting33}@163.com; zhanghao@ouc.edu.cn; agullive@ece.uvic.ca

Abstract—Accurate localization has gained significant interests in the field of ranging, locating and tracking systems. Impulse Radio (IR) 60GHz signal is practically operated in the literature, because of its high resolution of time and multipath. In order to improve the precision of the Time of Arrival (TOA) estimation, a threshold selection algorithm based on a joint metric of the skewness and kurtosis after energy detection is proposed in this paper. In addition, the optimal normalized threshold based on signal-to-noise ratio (SNR) is investigated, and the effects of integration period as well as channel model are validated. Then the performance under IEEE 802.15.3c Line of Sight (LOS) and None Line of Sight (NLOS) channel models is evaluated respectively. The results show that the proposed threshold selection algorithm is able to provide higher precision and robustness for TOA estimation over a long range of SNR in the 60GHz ranging system.

Index Terms—TOA, kurtosis, skewness, 60GHz, energy detection

I. INTRODUCTION

With the apparent advantages such as several GHz unlicensed spectrums, up to 10W maximum transmit power, low-cost Complementary Metal Oxide Semiconductor (CMOS) devices implement, high time and multipath resolution and so forth, the 60 GHz signal has become the first choice for short-range wireless communications [1]-[5]. The 60 GHz signal usually has a very short duration (typically 100 picoseconds or less). Therefore, the multipath signal can be separated at the receiving end effectively, which can lead to a higher multipath resolution. The accuracy with 60Hz positioning technology can up to the millimeter.

Generally, positioning technology can be classified into two categories: range based technology and non-range based technology. For range based technology, several classical methods have been applied practically, involving Time of Arrival (TOA) [6]-[8], and Time Different of Arrival (TDOA) [9]. While, non-range based technology includes the Received Signal Strength (RSS) and Angle of Arrival (AOA). However, range based technology (TOA or TDOA) could cooperate with 60GHz signal better, as it is capable of making full advantage of the high time resolution provided by the very short 60GHz pulses. Thus, we utilized TOA in this paper as the target locating technology. Furthermore, acquiring the ability of precise ranging demands accurate TOA estimation, but it could be challenging due to the potential hundreds of multipath components in 60GHz ranging system.

According to the ways of signal-receiving, TOA estimation can be divided into two types, Matched Filter (MF) [10] and Energy Detector (ED) [11]-[12]. A MF receiver usually requires higher sampling rate and higher correlation, such as a RAKE receiver. On the contrary, an ED receiver doesn't need a correlative template, which resulting in lower sampling rate and lower complex. Because of lower complex and higher convenience, ED is exploited during the TOA estimation in this paper.

In ED, the major problem is selecting a suitable threshold based on the received signal. In [13], a normalized threshold algorithm was proposed which using the minimum and maximum sample values. In [14], a normalized threshold selection algorithm for TOA estimation of UWB（Ultra-Wide Band）signals which are exploiting the Skewness of the received signal was proposed. In [15], a method using fixed threshold value to estimate the TOA delay was applied. Threshold selection for different SNR values was investigated via simulation. These approaches have limited TOA precision, as the strongest path is usually not the first arriving path because of None Line of Sight (NLOS) fading environments.

The novelty of our work mainly lies on the following two aspects:

1). The statistic characteristics of received signal including Kurtosis, Skewness, Maximum Slope and Standard Deviation, have been calculated to understand the negative influences on signal caused by the channel environment. Then, by integration analysis of signal features, mainly Skewness and Kurtosis, a threshold

selection algorithm was proposed for TOA estimation in 60GHz ranging system. The proposed method is able to mitigate the negative environmental effects and to improve the positioning precision and robustness for TOA estimation.

2). Based on our new threshold selection algorithm, several parameterization functions have been established to determine the relationship between joint metric of skewness and kurtosis and optimal normalized threshold values. The functions make it possible that the threshold is capable of being modified adaptively in response to the change of received signal, which indicates our algorithm is more sensitive to the environment and could response more effectively.

The remainder of this paper is organized as follows. The system model is introduced in Section 2, and the TOA estimation algorithm based on ED is introduced in Section 3. In Section 4, the characteristics of the statistical parameters are analyzed. Then, a threshold selection algorithm based on the Skewness and Kurtosis is proposed in Section 5. The performance results and discussion are presented in Section 6. Finally, Section 7 concludes the paper.

II. System Model

Currently, there are two important standards that have been developed for the 60 GHz wireless communications systems, IEEE 802.15.3c and IEEE 802.11ad [16]-[17]. In this paper, channel models in IEEE 802.15.3c standard are used because it is specifically designed for the wireless personal area networks and thus encompasses typical indoor environments. Further, IEEE 802.15.3c standard was developed for high data rate short-range wireless systems, so it is widely employed for the 60 GHz systems. The physical layer was designed to support transmission of data within a few meters at a maximum data rate of 2 Gbps. These models have been developed for communications in the frequency band 57 to 66 GHz in indoor residential, indoor office and library environments (with differences largely due to LOS and NLOS characteristics) [18]-[21]. In this paper, CM1.1 (residential LOS) and CM2.1 (residential NLOS) are applied and a Pulse Position Modulation Time Hopping 60GHz（PPM-TH 60GHz）signal is used. In this section, the 60GHz signal, multipath fading channel, as well as the ED is introduced.

A. The Transmitted 60GHz Signal

The transmitted 60 GHz signal has a very short duration (typically 100 picoseconds or less), and can be expressed as：

$$s(t) = \sum_{-\infty}^{+\infty} p(t - jT_f - C_j T_c - \alpha_j \varepsilon) \qquad (1)$$

where j and T_f are the frame index and frame duration. C_j is the pseudorandom integer-valued sequence. T_c is the chip duration. ε is the PPM time shift with the

data α_j either 0 or 1. If $\alpha_j = 1$, the signal will be shifted in time, otherwise there is no PPM shift. Here, $p(t)$ is given by:

$$p(t) = \frac{\sqrt{2}}{\beta} \exp\left(-2\pi \frac{t^2}{\beta^2}\right) \cos(2\pi f_c t) \qquad (2)$$

where β is the shape factor and f_c is the carrier frequency. In this paper, $\beta = 0.25e - 9$ and $f_c = 60GHz$. Fig. 1 shows the waveform of the IR-60GHz signal.
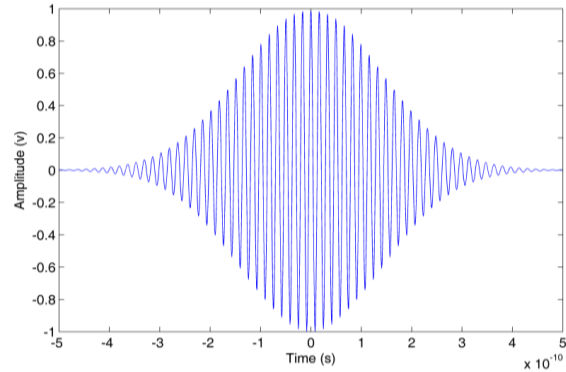
Fig. 1. Waveform of IR-60GHz signal

B. Multipath Fading Channel

Considering the influence caused by the multipath fading channel between the transmitter and receiver, the received signal is given by:

$$r(t) = \sum_{n=1}^{N} A_n p(t - \tau_n) + n(t) \qquad (3)$$

where N is the number of the received multipath components. A_n is the amplitude attenuation, and τ_n is the time delay of the nth path. $n(t)$ is the additive white Gaussian noise（AWGN）with zero mean and two-side power spectral density $N_0/2$.

In addition, (3) can be written as:

$$r(t) = s(t) * h(t) + n(t) \qquad (4)$$

where $s(t)$ is the transmitted 60GHz signal, $h(t, \theta)$ is the channel impulse realization, expressed as:

$$h(t, \theta) = \sum_{k=1}^{K} \sum_{l=1}^{L_k} \alpha_{kl} \delta(t - T_k - \tau_{kl}) \delta(\theta - \theta_k - \omega_{kl}) \qquad (5)$$

where $\delta(\cdot)$ expresses impulse function, K expresses the number of cluster arriving the receiver, L_k expresses the number of multipath in the kth cluster. α_{kl}, τ_{kl} and ω_{kl} express the plural amplitude value, delay and arrival angle in the kth cluster, lth path respectively. T_k and θ_k express the delay and arrival angle in the kth cluster.

C. Energy Detector

As shown in Fig. 2, after the amplifier, the received signals are squared, and then input to an integrator with integration period T_b. After that, the threshold is applied before the TOA estimation.
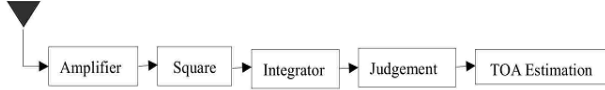
Fig. 2. Energy detection receiver

The integration period is set up to T_b, so the integrator output is given by:

$$z[n] = \sum_{j=1}^{N_s} \int_{(j-1)T_f+(c_j+n-1)Tb}^{(j-1)T_f+(c_j+n)Tb} r^2(t)dt \qquad (6)$$

where $n \in \{1, 2, ..., N_b\}$, which denotes the sample index with respect to the starting point of the uncertainty region. N_b represents the total number of the energy blocks. In this paper, N_s=1, i.e., the number of pulses per symbol is 1. So (6) can be rewritten as follows:

$$z[n] = \int_{(c_j+n-1)Tb}^{(c_j+n)Tb} r^2(t)dt \qquad (7)$$

If the received signal contains noise only, z[n] obeys centralized Chi-square distribution. However, if there are noise and signal, z[n] obeys non-centralized Chi-square distribution. The means and variances are given by:

$$\mu_0 = F\sigma^2, \sigma_0^2 = 2F\sigma^4 \qquad (8)$$

$$\mu_\varepsilon = F\sigma^2 + E_n, \sigma_\varepsilon^2 = 2F\sigma^4 + 4\sigma^2 E_n \qquad (9)$$

where F is the degree of freedom given by $F = 2BT_b + 1$. E_n is the total signal energy within the whole nth block, and B is the signal bandwidth.

III. TOA ESTIMATION

A. TOA Estimation Algorithm

There are many TOA estimation algorithms based on ED for determining the start block of a received signal. The simplest algorithm is the Maximum Energy Selection (MES), which chooses the maximum energy value as the start of the signal. The TOA is estimated as the center of corresponding integration period, and the TOA estimation of MES is given by:

$$\tau_{MES} = [\arg\max_{1 \le n \le n_b}\{n \mid z[n]\} - 0.5]T_b \qquad (10)$$

However, the maximum energy value may not be the first energy block, especially in NLOS environments. On average, the first energy value z[n] is received before the maximum energy value $z[n_{max}]$, i.e. $n < n_{max}$. Thus, the Threshold-Crossing (TC) TOA estimation is proposed, where the received energy values are compared to an appropriate threshold ξ. The TOA estimation is given by:

$$\tau_{TC} = [\arg\min_{1 \le n \le n_{max}}\{n \mid z[n] \ge \xi\} - 0.5]T_b \qquad (11)$$

So the problem is how to set up an appropriate threshold ξ. It is difficult to determine ξ directly, so a normalized threshold ξ_{norm} is applied. The relationship between ξ and ξ_{norm} is given by:

$$\xi = \xi_{norm}(\max(z(n)) - \min(z(n))) + \min(z(n)) \qquad (12)$$

Then, the τ_{TC} is obtained via (11).

B. Error Analysis of TOA Estimation Algorithm

In [8], the Mean Absolute Error (MAE) of TC-based TOA estimation was analyzed, and closed form error expressions derived. The MAE is used to evaluate the quality of an algorithm and is expressed as:

$$MAE = \frac{1}{N}\sum_{n=1}^{N} |t_n - \hat{t}_n| \qquad (13)$$

where t_n is the nth true TOA. $\hat{t}_n$ is the nth TOA estimation. N is the number of TOA estimation.

IV. STATISTICAL CHARACTERISTICS OF THE RECEIVED SIGNAL

During the ranging process, the threshold selection algorithm aims to provide a method to find the accurate time when the integrator outputs z[n] is obtained. Analyzing the statistical characteristics of z[n] could help us building a suitable relationship between z[n] and threshold selection algorithm. In this section, signals under IEEE 802.15.3c CM1.1 and CM2.1 channels are simulated, and parameters such as Skewness, Kurtosis, Maximum Slope and Standard Deviation are analyzed.

A. Kurtosis

Kurtosis (K) is used to describe the steepness of the energy blocks. For a standard distribution, the value of Kurtosis is three. Thus, K is often defined as K=K-3, named excess Kurtosis. K is given by:

$$K = \frac{1}{(N-1)\delta^4}\sum_{i=1}^{N}(x_i - \bar{x})^4 - 3 \qquad (14)$$

where $\bar{x}$ and δ are the mean and standard deviation of the energy block values. For noise only (or for a low SNR) and sufficiently large F (degree of freedom of the Chi-square distribution), z[n] obeys Gaussian distribution and K=0. Otherwise, K increases as the SNR increases.

B. Skewness

Skweness (S) is used to describe the distribution symmetry of the whole value and is given by:

$$S = \frac{1}{(N-1)\delta^3}\sum_{i=1}^{N}(x_i - \bar{x})^3 \qquad (15)$$

where $\bar{x}$ and δ are the mean and standard deviation of the energy block values. For noise only (or for a low SNR) and sufficiently large F, S=0. Otherwise, S will increase as the SNR increases.

C. Standard Deviation

Standard Deviation shows the data's discrete degree from the average. It is given by:

$$D = \sqrt{\frac{\sum_{i=1}^{N}(x_i - \bar{x})^2}{N-1}} \qquad (16)$$

D. Maximum Slope

Maximum Slope is used to analyze the slope of energy blocks. All energy blocks are divided into (N-M+1) groups, with each group contains M energy blocks. Every slope of each group is calculated using a least squares line fit. It is given by:

$$M = \max_{1 \leq n \leq N-M+1} \{linefit(z[n], z[n+1],...,z[n+M-1])\} \quad (17)$$

E. Statistical Characteristics of Four Parameters

In order to analyze the characteristics of the four parameters (Kurtosis, Skewness, Standard Deviation and Maximum Slope), signals under the CM1.1 and CM2.1 channel models of the IEEE 802.15.3c are simulated. And for each SNR, there are 1000 channel responses. In addition, the signal propagation delay is 0-T_f. Other parameters are: $f_c = 60\text{GHz}$, $T_f = 200\text{ns}$, $T_c = 1\text{ns}$, $T_b = 4\text{ns}$, $N_s = 1$, and $f_s = 60.5\text{GHz}$, where f_c is the center frequency of the transmitted 60GHz signal, T_f is the frame duration, T_c is the chip duration, T_b is the integration period, N_s is the number of pulses per symbol, f_s is the sample frequency.
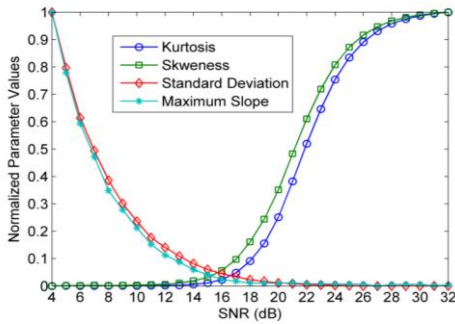
Fig. 3. Normalized statistical parameters of $z[n]$ via CM1.1
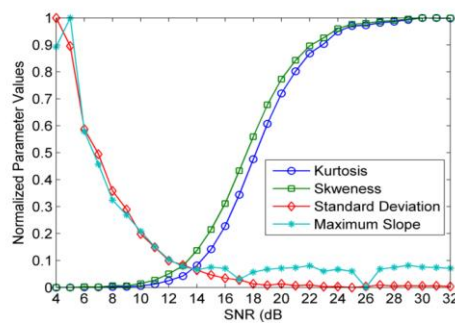
Fig. 4. Normalized statistical parameters of $z[n]$ via CM2.1

The simulations of the four statistical parameters are showed in Fig. 3 and Fig. 4. The figures present that the Kurtosis and Skewness tend to increases as the SNR increases, but the Skweness changes more rapidly. On the contrary, the Standard Deviation and Maximum Slope decrease as the SNR increases, but the changing trend is different for CM1.1 and CM2.1. In CM1.1, the Maximum Slope changes more rapidly than the Standard Deviation, while in CM2.1, it is just the opposite. Through the experimental data, we find that the original values of the

Standard Deviation are too small, and the Maximum Slope values under CM1.1 are quite different from the values under CM2.1. So they are both unrealistic to be the standard of the threshold selection algorithm. Moreover, when SNR is less than 14dB, there is no obvious change on Skewness and Kurtosis. No single parameter is a good measure of SNR change over a wide range of values. Thereby, we take the Skewness and Kurtosis into consideration.
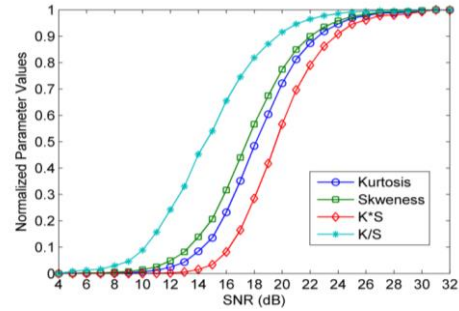
Fig. 5. Normalized statistical parameters via CM1.1
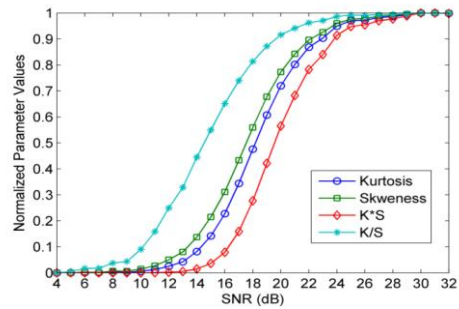
Fig. 6. Normalized statistical parameters via CM2.1

Here, K*S and K/S represent the multiplication and division of the Kurtosis and Skewness, respectively. In this paper, K, S, K*S and K/S, were calculated, and the results are showed in Fig. 5 and Fig. 6. For four parameters, the K/S changes more rapidly than the others. In other words, K/S better reflects the changes in SNR, and so more suitable for TOA estimation. Fig. 5 and Fig. 6 also show that the values under CM1.1 are similar to that of CM2.1, so the joint metric is insensitive to channel models. Taking K/S as the standard to set up threshold values could combine the differences between LOS and NLOS paths. Thus, a joint metric based on the K/S is proposed in Section 5.

V. THRESHOLD SELECTION BASED ON SKEWNESS AND KURTOSIS

A. Joint Metric J

The joint metric is given by:

$$J = K / S \quad (18)$$

where K is the Kurtosis, S is the Skewness.

In order to verify the relationship between J and SNR, 1000 channel realizations were generated in each IEEE802.15.3c CM1.1 and CM2.1 channels. The result is showed in Fig. 7. It presents that J is a monotonic

function with high sensitivity for a large range of SNR values, especially between 8dB to 20dB. As situations with too low or too high SNR are not common in practical, so taking *J* as the standard is of realistic significance. The Fig. 7 shows that the relationship between *J* and SNR is not affected by the channel models significantly. It is more related to integration periods than channel models.

B. Threshold Selection Based on J

In order to utilize advantages of the Joint Metric J, threshold selection algorithm aims to find relationship between J and the best threshold (ζ_{best}). There is no direct connection between J and ζ_{best}, but intermediate variable SNR could be used. The procedures are as follows:

1. Build relationship between J and SNR, which we have showed in Fig. 7.
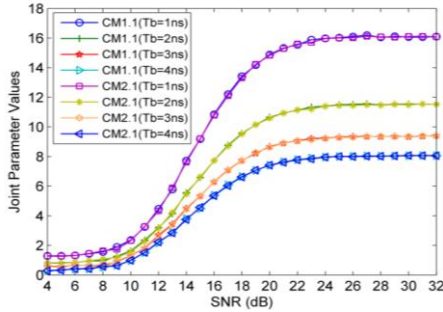
Fig. 7. Joint values with SNR for different CM and T_b.

2. Build relationship between ζ_{best} and SNR. However, SNR could not be associated with ζ_{best} directly. It is well known that the normalized threshold (ζ_{norm}) could be the ζ_{best} when MAE takes the minimum value. According to this, following steps are used to build relationship between SNR and ζ_{best}.

1) Fix a ζ_{norm}, relationship between SNR and MAE could be built by simulation directly.

2) Change the value of ζ_{norm} ($\zeta_{norm} \in \{0.1, 0.2, ..., 0.9\}$), find the corresponding relationship between SNR and MAE.

3) Present the nine relation curve in one figure, just as the Fig. 8- Fig. 15.
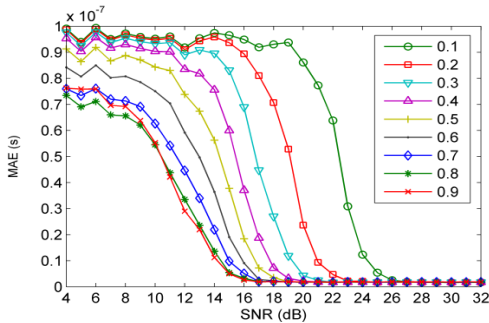
Fig. 8. MAE with SNR (CM1.1, T_b=4ns).

4) Find relationship between SNR and ζ_{best}. Taking Fig. 8 as an example, with a certain SNR, ζ_{best} is the ζ_{norm}

when MAE takes the minimum value. Then the relationship between SNR and ζ_{best} is found.
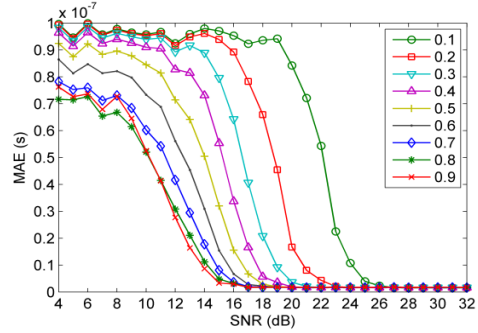
Fig. 9. MAE with SNR (CM1.1, T_b=3ns).
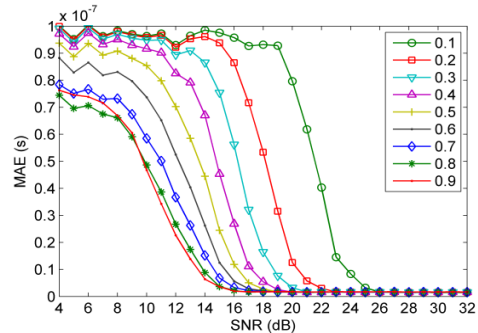
Fig. 10. MAE with SNR (CM1.1, T_b=2ns).
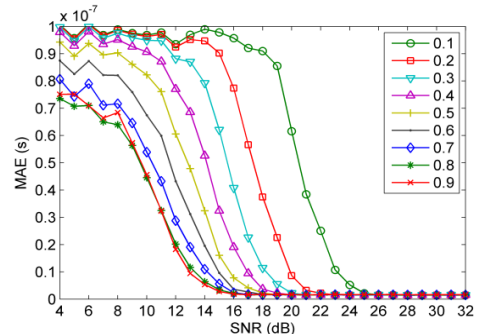
Fig. 11. MAE with SNR (CM1.1, T_b=1ns).

3. Build relationship between ζ_{best} and J. Since relationships between J and SNR, as well as ζ_{best} and SNR are found in steps 1 and 2, it is simple to associate ζ_{best} with J.

4. Use Curve Fitting to establish function between ζ_{best} and J. Four functions for $T_b = 4$ ns, 3 ns, 2 ns, 1 ns, are given in (20) -(23).
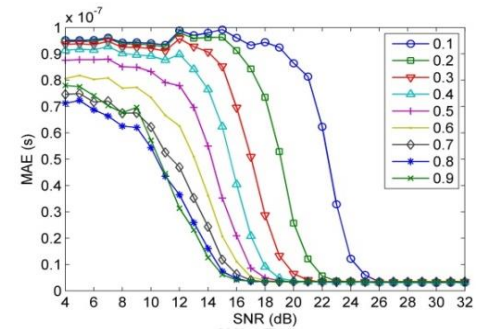
Fig. 12. MAE with SNR (CM2.1, T_b=4ns).
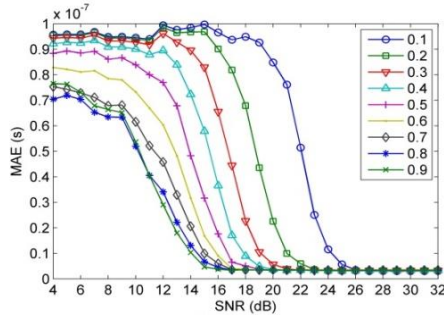
Fig. 13. MAE with SNR (CM2.1, T_b=3ns).
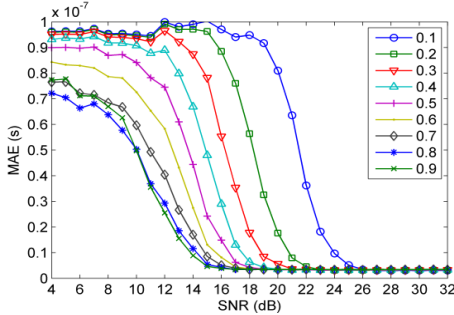
Fig. 14. MAE with SNR (CM2.1, T_b=2ns).
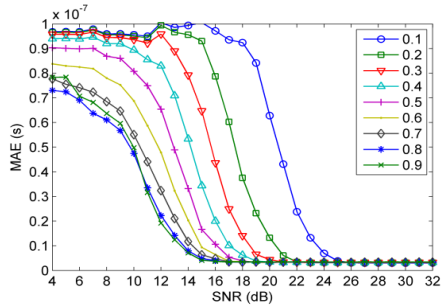
Fig. 15. MAE with SNR (CM2.1, T_b=1ns).

To verify the algorithm, 1000 times realizations for CM1.1 and CM2.1 channel were simulated. Fig. 8-Fig. 15 show MAE for $\xi_{norm} \in \{0.1, 0.2, ..., 0.9\}$ in the CM1.1 and CM2.1 channels with $T_b = 4ns, 3ns, 2ns, 1ns$ respectively. According to the curves, the tendency could be revealed that MAE decreases in response to the declination of SNR, and vice versa. In addition to the fact investigated before that J is proportional to SNR, the relationship between J and MAE could also be determined where MAE varies rightly opposite to the change of J. However, when SNR was assigned by extremely large value, MAE tends to stay consistent and remain stable.

Since J is more closely related to the integration periods rather than transmitting channel models, and in order to get the optimal expected value, we suggest that ζ_{best} should be obtained by taking average of the two values, which are acquired separately over the CM1.1 and CM2.1 channels. This method is expressed as (19).

$$\xi_{best}^{(Tb=xns)}(J) =$$
$$\frac{\xi_{best}^{(CM1.1,Tb=xns)}(J) + \xi_{best}^{(CM2.1,Tb=xns)}(J)}{2} (x = 1,2,3,4) \quad (19)$$

In order to find the relationship between ζ_{best} and J, Curve Fitting is used. The results are showed in Fig. 16 to Fig. 19. Four functions for $T_b = 4$ ns, 3 ns, 2 ns, 1 ns, are given in (20) -(23).

$$\xi_{best}^{(1ns)}(J) = \begin{cases} 0.8, J < 2 \\ -0.007976*exp(0.3117*J) + \\ 0.7923*exp(0.03123*J), 2 \le J \le 16 \\ 0.1, J > 16 \end{cases} \quad (20)$$

$$\xi_{best}^{(2ns)}(J) = \begin{cases} 0.8, J < 1 \\ -0.002011*exp(0.5446*J) + \\ 0.7947*exp(0.03421*J), 2 \le J \le 11.4 \\ 0.1, J > 11.4 \end{cases} \quad (21)$$

$$\xi_{best}^{(3ns)}(J) = \begin{cases} 0.825, J < 2 \\ -0.0001155*exp(0.9603*J) + \\ 0.81*exp(0.02614*J), 2 \le J \le 9.3 \\ 0.1, J > 9.3 \end{cases} \quad (22)$$

$$\xi_{best}^{(4ns)}(J) = \begin{cases} 0.8, J < 0.6 \\ -0.001768*exp(0.7972*J) + \\ 0.7806*exp(0.05364*J), 0.6 \le J \le 8.03 \\ 0.1, J > 8.03 \end{cases} \quad (23)$$
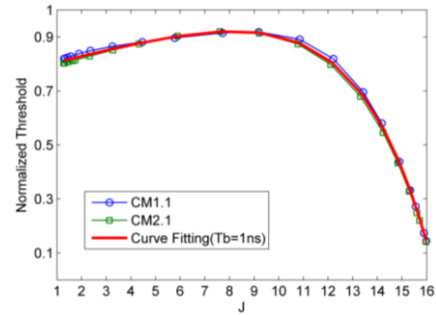
Fig. 16. Best normalized threshold with J (T_b=1ns)
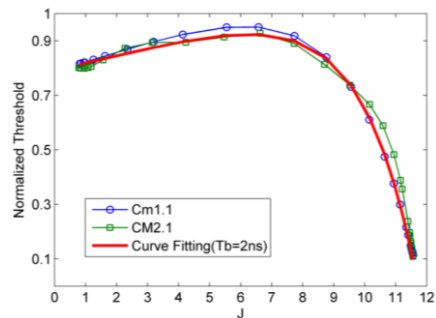
Fig. 17. Best normalized threshold with J (T_b=2ns)
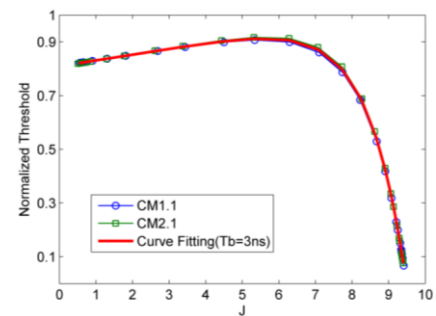
Fig. 18. Best normalized threshold with J (T_b=3ns)
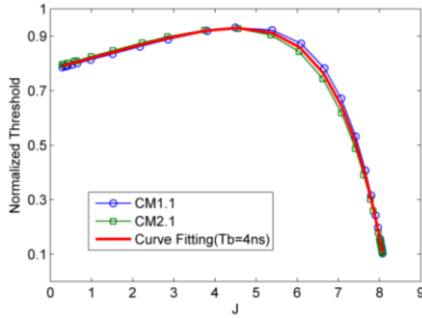
Fig. 19. Best normalized threshold with *J* (T_b=4ns)

VI. PERFORMANCE AND DISCUSSION

MAEs were examined for different TOA estimation algorithms based on Energy Detection in the IEEE 802.15.3c CM1.1 and CM1.2 channels with Tb=1ns, 2ns, 3ns, 4ns. For each algorithm, 1000 times channel realizations have been simulated. The main system parameters were set up as: $f_c = 60\text{GHz}$, $T_f = 200\text{ns}$, $T_c = 1\text{ns}$, $N_s = 1$, and $T_b = 1$ ns, 2 ns, 3 ns, and 4 ns.

Each realization had a TOA uniformly distributed with (0-Tf). In addition, the experimental data with Tb=2ns and Tb=3ns are between Tb=1ns and Tb=4ns, and the changing trend with Tb=2ns and Tb=3ns is similar to Tb=1ns and Tb=4ns.

In addition, the experimental data acquired under the condition of T_b=1ns and T_b=4ns is able to represent all potential value that might be generated by simulations in this paper. What is more, all four possible Tb have the same change tendency which could be illustrated by given pictures.

Thus, in order to simplify and clarify the test result , we decided to take Tb=1ns and Tb=4ns as examples to evaluate the system performance.
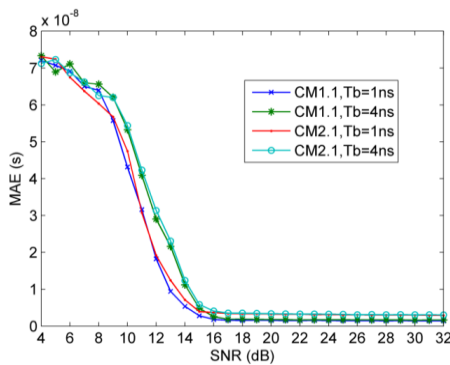
Fig. 20. MAE for CM1.1 and CM2.1 (T_b=1ns and T_b=4ns)

Based on the Joint Metric *J* that we proposed, Fig. 20 presents the TOA estimation MAE for SNR in CM1.1 and CM2.1 with T_b=1ns and T_b=4ns. From the picture, we gain that the algorithm based on *J* performs well at high SNR. MAE is more related to channel models than integration periods. When SNR>16dB, the MAE for CM1.1 and CM2.1 is about 1.5ns and 3ns. The positioning precision is given by:

$$d = c\tau_{TC} \qquad (24)$$

where *c* is the propagation speed, and τ_{TC} is the TOA estimation. In this paper, c is 3e8 meters per second.

Thus, the positioning precision can reach to 0.45 meter for CM1.1 and 0.9 meter for CM2.1. So, the precision in CM1.1 is higher than in CM2.1. Moreover, when SNR<16dB, the MAE with T_b=1ns is lower than T_b=4ns in both CM1.1 and CM2.1 channels.

Fig. 21-Fig. 22 displays the MAE performance of three TOA algorithms in CM1.1 and CM2.1 channels, respectively. The threshold in the Fixed-Threshold (FT) algorithm was arranged to a fixed value (0.4); the maximum energy value was chosen as the start of the signal value for the Maximum Energy Selection (MES); and an assumed optimal threshold was generated by the Joint Metric in the proposed algorithm based on Kurtosis and Skewness. As we expected, the new Joint Metric algorithm earns the lowest value of MAE , particularly at low or moderate range of SNR in both CM1.1 and CM2.1 channels with both situation Tb=1ns and Tb=4ns. For example, for CM1.1 with Tb=1ns and SNR=4dB to 14dB, the MAE of the proposed algorithm is better by 8ns~18ns than MES. However, when the SNR is great than 20dB, there is almost no difference for each algorithm. Take situation that SNR exceeds 14dB as instance, there is only 1ns advantage between compared algorithms. In a result, the proposed threshold selection algorithm is particularly suitable for communication environment with low or moderate SNR. As the majority of real transmitting channels are characterized by low or median SNR, our proposed algorithm could be more plausible for practical usage than traditional methods.
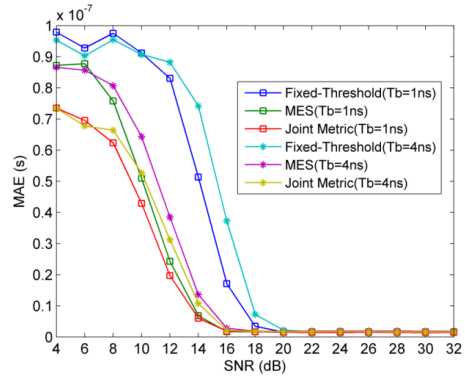
Fig. 21. MAE for different algorithm with CM1.1
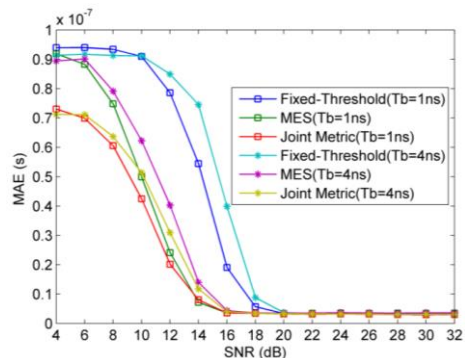
Fig. 22. MAE for different algorithm with CM2.1

VII. CONCLUSIONS

This paper analyzes the characteristics of received 60 GHz signals under 802.15.3c CM1.1 and CM2.1 channel models. According to extensive simulations, a new threshold selection algorithm for TOA estimation based on Kurtosis and Skewness in IR-60GHz ranging system is proposed. In order to analyze the performance of the proposed algorithm, the MAE is used to describe the effects caused by the integration period and channel model. The result shows that the effect of the channel model on the proposed algorithm is smaller than that of integration period. The proposed threshold selection algorithm has higher positioning precision than other traditional methods, especially under the situations with low or moderate SNR. Furthermore, using curve fitting, the best normalized threshold was simulated over the CM1.1 and CM2.1 channels. And functions used to describe the relationship between joint metric and best normalized threshold are summarized. Based on the functions, threshold values can be changed with the received signals timely. It means that the proposed threshold selection algorithm provides higher robustness and positioning precision than several other algorithms.

ACKNOWLEDGMENT

REFERENCES

[1] G. Nan, "60-GHz millimeter-wave radio: Principle, technology, and new results," *Eurasip Journal on Wireless Communications & Networking*, pp.211-216, Jan. 2007.

[2] L. Zhang, "A fully integrated 60GHz four channel CMOS receiver with 7GHz ultra-wide band width for IEEE 802.11ad standard," *Communication*, China, vol. 11, no. 6, pp. 42-50, 2014.

[3] S. K. Yong, P. F. Xia, and V. G. Alberto, "60-GHz strategy for gbps WLAN and WPAN: From theory to practice," *Press of China Machine*, Beijing, 2013.

[4] R. C. Daniels and R. W. Heath, "60 GHz wireless communications: Emerging requirements and design recommendation," *IEEE Vehicular Technology Magazine*, vol. 2, no. 3, pp. 41-50, 2007.

[5] C. P. Yen and P. J. Voltz, "Indoor positioning based on statistical multipath channel modeling," *EURASIP Journal on Wireless Communications and Networking*, vol. 1, pp. 1-19, 2011.

[6] D. Amico, A. A. U. Mengali, and L. Taponecco, "Energy-Based TOA estimation," *IEEE Transactions on Wireless Communications*, vol. 7, no. 3, pp. 838-847, 2008.

[7] W. Liu, H. Ding, and X. Huang, "TOA estimation in IR UWB ranging with energy detection receiver using received signal characteristics," *IEEE Communications Letters*, vol. 16, no. 5, pp. 738-741, 2012.

[8] A. Eva, J. J. Murillo-Fuentes, and R. Boloix-Tortosa, "Blind low complexity time-of-arrival estimation algorithm for UWB signals," *IEEE Signal Processing Letters*, vol. 22, pp. 2019-2023, 2015.

[9] M. Bocquet, C. Loyez, and A. Benlarbi-Delai, "Using Enhanced-TDOA measurement for indoor positioning," *IEEE, Microwave and Wireless Components Letters*, vol. 15, no. 10, pp. 612-614, 2005.

[10] Y. Z. Xu, E. K. S. Au, and K. S. Wong, "A novel threshold-based coherent TOA estimation for IR-UWB systems," *IEEE Trans. Vehicular Technology*, vol. 58, no. 8, pp. 4675-4681, 2009.

[11] C. Hong, T. Lv, and Y. Lu, "Decision feedback threshold selection for UWB TOA estimation with energy detection receiver," in *Proc. International Conference on Cyberspace Technology*, 2013, pp. 555-560.

[12] W. Y. Liu and X. Huang, "Analysis of energy detection receiver for TOA estimation in IR UWB ranging and a novel TOA estimation approach," *Journal of Electromagnetic Waves & Applications*, vol. 28, no. 1, pp. 49-63, 2014.

[13] I. Guvenc and Z. Sahinoglu, "Threshold-Based TOA estimation for impulse radio UWB systems," in *Proc. International Conference on Ultra-Wideband*, 2005, pp. 420-425.

[14] X. Cui, H. Zhang, and T. A. Gulliver, "Threshold selection for ultra-wideband TOA estimation based on neural networks," *Journal of Networks*, vol. 7, no. 9, pp. 1311-1318, 2012.

[15] C. Hong, "TOA estimation using checking Window for IR-UWB energy detection receivers," *IEEE 79th Vehicular Technology Conference*, 2014, pp. 1-5.

[16] IEEE Standard for Information Strategy--Local and Metropolitan Area Networks--Specific Requirements, Part 15.3: Wireless Medium Access Control (MAC) and Physical Layer (PHY) Specifications for High Rate Wireless Personal Area Networks (WPAN) Amendment 2: Millimeter-Wave-Based Alternative Physical Layer Extension, IEEE Computer Society, IEEE 802.15.06-0474-00-003c. New York, USA, 2009.

[17] 802.11n-2009-IEEE Standard for Information Strategy--Local and Metropolitan area Networks--Part 11: Wireless LAN Medium Access Control (MAC)and Physical Layer (PHY) Specifications Amendment 5: Enhancements for Higher Throughput, IEEE Computer Society, IEEE 978-0-7381-6731-2. New York, USA, 2009.

[18] T. Redant and W. Dehaene, "An MLS-Prony implementation for a cm-Precise Super 10 m range 802.15.3c-PHY 60 GHz positioning application," *Journal of Ambient Intelligence and Humanized Computing*, vol. 5, no. 5, pp. 623-634, 2014.

[19] V. Savicl, "Measurement analysis and channel modeling for TOA-Based ranging in tunnels," *IEEE Transactions on Wireless Communications*, vol. 14, pp. 49-63, 2014.

[20] M. P. Wylie and J. Holtzman, "The non-line of sight problem in mobile location estimation," in *Proc. 5th IEEE International Conference on Universal Personal Communications*, 1996, pp. 827-831

[21] T. Baykas, C. S. Sum, and Z. Lan, "IEEE 802.15. 3c: The first IEEE wireless standard for data rates over 1 Gb/s," *Communications Magazine*, vol. 49, no. 7, pp. 114-121, 2011.

Ning Du was born in Shandong, China, in 1991. She received her B.S. degree of communication engineering in Ocean University of China, Qingdao, China, in 2014. From 2014 to now, she is pursuing the M.S. degree with the Department of Electrical Engineering in Ocean University of China. Her research interests include UWB and 60 GHz wireless communication and positioning.

Hao Zhang was born in Jiangsu, China, in 1975. He received his Bachelor Degree in Telecom Engineering and Industrial Management from Shanghai Jiaotong University, China in 1994, his MBA from New York Institute of Technology, USA in 2001, and his Ph.D. in Electrical and Computer Engineering from the University of Victoria, Canada in 2004. In 2000, he joined Microsoft Canada as a Software Engineer, and was Chief Engineer at Dream Access Information Technology, Canada

from 2001 to 2002. He is currently a professor in the Department of Electrical Engineering at the Ocean University of China, and an Adjunct Assistant Professor in the Department of Electrical and Computer Engineering at the University of Victoria. His research interests include UWB wireless systems, MIMO wireless systems, and spectrum communications.

Tingting Lv received the Ph. D. degree in College of Information Science and Engineering from Ocean University of China in 2013. She received her Master Degree in the Department of Electrical Engineering in Ocean University of China in 2009, and B.S. Degree in College of HuNan University in 2006. She was born in 1983. She is currently a lecture in the Department of Electrical Engineering at the Ocean University of China. Her research interests include ultra-wideband radio systems, 60GHz wireless communication system.

T. Aaron Gulliver received the Ph. D. degree in Electrical and Computer Engineering from the University of Victoria, Canada in 1989. He is now a professor and the Ph. D. supervisor in the Department of Electrical and Computer Engineering. In 2002, he becomes a Fellow of the Engineering Institute of Canada, and in 2012 a Fellow of the Canadian Academy of Engineering. He is also a senior member of IEEE. His research concerns information theory and communication theory, algebraic coding theory and smart grid and ultra-wideband communication